Nanoscale Res Lett (2008) 3:158–163
DOI 10.1007/s11671-008-9130-8

NANO EXPRESS

Cathodoluminescence and Cross-sectional Transmission Electron Microscopy Studies for Deformation Behaviors of GaN Thin Films Under Berkovich Nanoindentation

Sheng-Rui Jian · I-Ju Teng · Jian-Ming Lu

Received: 4 March 2008 / Accepted: 4 April 2008 / Published online: 15 April 2008
© to the authors 2008

Abstract In this study, details of Berkovich nanoindentation-induced mechanical deformation mechanisms of metal-organic chemical-vapor deposition-derived GaN thin films have been systematic investigated with the aid of the cathodoluminescence (CL) and the cross-sectional transmission electron microscopy (XTEM) techniques. The multiple “pop-in” events were observed in the load-displacement (*P*–*h*) curve and appeared to occur randomly by increasing the indentation load. These instabilities are attributed to the dislocation nucleation and propagation. The CL images of nanoindentation show very well-defined rosette structures with the hexagonal system and, clearly display the distribution of deformation-induced extended defects/dislocations which affect CL emission. By using focused ion beam milling to accurately position the cross-section of an indented area, XTEM results demonstrate that the major plastic deformation is taking place through the propagation of dislocations. The present observations are in support to the massive dislocations activities occurring underneath the indenter during the loading cycle. No evidence of either phase transformation or formation of micro-cracking was observed by means of scanning electron microscopy and XTEM observations. We also discuss how these features correlate with Berkovich nanoindentation produced defects/dislocations structures.

Keywords GaN · MOCVD · Nanoindentation · Cathodoluminescence · Focused ion beam · Transmission electron microscopy

S.-R. Jian (✉)
Department of Materials Science and Engineering,
I-Shou University, Kaohsiung 840, Taiwan
e-mail: srjian@gmail.com

I.-J. Teng
Department of Materials Science and Engineering,
National Chiao Tung University, Hsinchu 300, Taiwan

J.-M. Lu
National Center for High-Performance Computing,
National Applied Research Laboratories, No. 28, Nanke 3rd Rd.,
Sinshih Township, Tainan County 74147, Taiwan

Introduction

As one of the groups III–V nitride semiconductors, GaN is a highly attractive material because of its great potential for development of optoelectronic devices in short-wave length, semiconductor lasers, and optical detectors [1, 2]. The compound exhibits some interesting characteristics, such as larger band gap, strong interatomic bonds, and high thermal conductivity, which make it to be fine materials for optoelectronic, high-temperature and high-power devices. Nevertheless, the successful fabrication of devices based on epitaxial GaN thin films requires better understanding of the mechanical characteristics in addition to its optical and electrical performances, since the contact loading during processing or packaging can significantly degrade the performance of these devices. Consequently, there is a growing demand of investigating the mechanical characteristics of materials, in particular in the nanoscale regime, for device applications.

The practical use of materials requires a knowledge of their mechanical behaviors and the effect of mechanical damage on their desired characterizations, because through the fabrication or handling processes the materials may be subjected to mechanical loads which cause damage, or the mechanical loads arise from shock loading in mobile systems. In this respect, the advent of nanoindentation instruments and the subsequent development of underlying

science may potentially address the scaling issue and the scientific evaluation of all contact loading-related phenomena. Since the deformation occurred during the test is controlled locally on the nanometer-scale, nanoindentation has, recently, been widely used to investigate the deformation mechanisms of various semiconductors [3–6]; as well as the mechanical characteristics of surfaces of solids and thin films, such as the hardness and Young's modulus, have been extracted using this technique [7–9].

We present herein the Berkovich nanoindentation-induced mechanical deformation mechanisms of the metal-organic chemical-vapor deposition (MOCVD)-derived GaN thin films by means of the cathodoluminescence (CL) microscopy in a scanning electron microscopy (SEM/CL) and the cross-sectional transmission electron microscopy (XTEM) techniques.

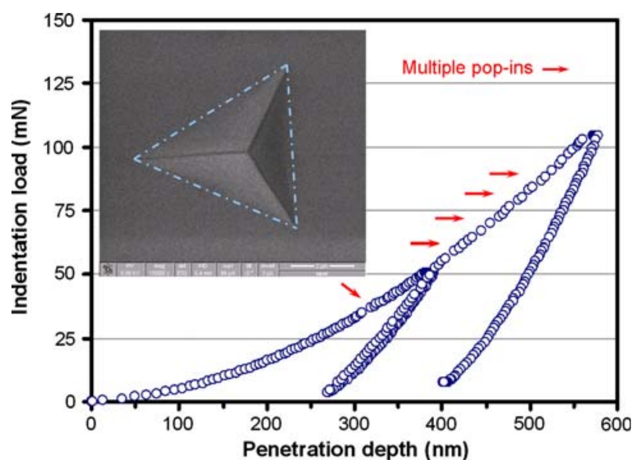

Fig. 1 Typical cyclic nanoindentation *P–h* curves for GaN thin films obtained with a Berkovich indenter. Results show the clear multiple "pop-in" events (indicated by the arrows) during loading, while no "pop-out" event is evident in the unloading segments, indicating that no phase transition is involved. The inset is an SEM micrograph of an indent at an applied load of 100 mN. No apparent material pile-up around the indented area is evident

Experimental Details

GaN thin films used in this work were grown on (0001)-sapphire substrates by using the MOCVD method with an average thickness of about 2 μm. The details of growth procedures in preparing these GaN thin films can be found elsewhere [10].

The nanoindentation measurements were performed on a Nanoindenter MTS NanoXP® system (MTS Cooperation, Nano Instruments Innovation Center, TN, USA) with a diamond pyramid-shaped Berkovich-type indenter tip, whose radius of curvature is 50 nm. The cyclic nanoindentation tests were performed in a way with loading to the maximum load and unloading by 90%; reloading to the maximum load and unloading by 9%; holding for 10 s at 10% of the maximum load for thermal drift correction and complete unloading, as illustrated in Fig. 1. The thermal drift was kept below ±0.05 nm/s for all indentations considered in this work. The same loading/unloading rate of 10 mN/s was used. At least 50 indents were performed on GaN thin films. The nanoindentations were sufficiently spaced to prevent from mutual interactions.

In addition, the hardness and Young's modulus of GaN thin films were measured by nanoindentation with a continuous stiffness measurements technique [11], and the indentations were made using a constant nominal strain rate of 0.05 s^{-1}. Frequency of 45 Hz was used to avoid the sensitivity to thermal drift and the loading resolution was 50 nN. In this technique, a harmonic force is superimposed to the nominal applied force. This oscillated force with a known phase and amplitude interacts with the material, which responds with a displacement phase and amplitude characteristic of the stiffness and damping of contact with the indenter. Consequently, the stiffness data along with the load and displacement curve are recorded. Hardness and Young's modulus of GaN thin films, calculated from the load-displacement (*P–h*) records by using the analytic method developed by Oliver and Pharr [12], are 19.3 ± 1.1 and 286.1 ± 25.3 GPa, respectively.

In our measurements, firstly, a 10 × 10-indentation array with each indentation being separated by 100 μm to avoid inter-indent interactions was produced with an indentation load of 100 mN. In each indentation tests, the Berkovich diamond indenter was operated with the same loading/unloading rate (10 mN/s) and was held at the peak load for 10 s.

After that, XTEM samples were prepared by the lift-out technique using a dual-beam focused ion beam (FIB) station (FEI Nova 220). The technique for material preparation using the FIB consisted of first milling two crosses alongside the indented area, acting as markers and then depositing a 1-μm thick layer of Pt to protect the area of interest from Ga^+ ion beam damage and implantation. Material was therefore removed from both sides of the selected area using an ion current of 5 nA, followed by successive thinning steps using decreasing currents from 3 nA to 300 pA until the lamella was about 1-μm thick. Subsequently, the bottom and one side of the lamella were cut-free while tilting the specimen at an angle of 45° to the ion beam. A central area containing the indentation apex of a few micrometers in length was then chosen and thinned further to a thickness of 100 nm, leaving at the sides thicker areas that prevented the lamella from collapsing. Finally, a small area of interest was selected and thinned until electron transparency was achieved. The transfer of the lamella from the sample holder to the TEM grid with a

carbon membrane was made ex situ using the electrostatic force of a glass needle. The XTEM lamella was examined in a JEOL 2010F TEM operating at 200 kV with a point-to-point resolution of 0.23 nm and a lattice resolution of 0.10 nm.

The room temperature CL measurement was performed using a Gata monocle equipped on the JEOL JSM-7000F field-emission SEM. A 20 keV electron beam energy level was selected to excite the sample.

Results and Discussion

The typical cyclic nanoindentation *P–h* curve of GaN thin films subjected to a maximum indentation load of 100 mN is illustrated in Fig. 1. The curve exhibits irregularities during loading characterized by small jumps in the penetration depth (see the arrows), referred to as the multiple "pop-in" events in what follows. The fact that multiple "pop-in" events are observable over such a wide range of indentation load and penetration depth indicates the close relations to the plastic deformation of GaN thin films. Furthermore, since the phenomena are randomly distributed on the loading curve and each curve is associated with a different stress rate which increases with the maximum indentation load, it is suggestive that the first "pop-in" event is not thermally activated. Dislocation-induced "pop-in" event is usually associated with two distinct deformation behaviors before (pure elastic behavior) and after (elasto-plastic behavior) the phenomena [13]. In this work, it cannot be provided for such indentation load any evidence of dislocation activity and crack features at the free surface around the indentation from SEM observations, as illustrated in the insert of Fig. 1. Also, no reversal discontinuities during unloading segment of *P–h* curves, commonly called the "pop-out" events are observed here; such phenomena are observed for instance in Si and related to phase transformation just beneath the diamond indenter [14, 15]. One possible mechanism that would explain the observed behavior is the formation and propagation of dislocations in GaN thin films.

After Berkovich nanoindentation, the residual indentations were directly imaged by using secondary electron (SE) and CL. A series of CL images of near-gap emission from GaN thin films indented to the maximum indentation loads of 10, 50, and 100 mN is shown in Figs. 2a–c, respectively. We clearly observe an indentation pattern called "rosette", with a structure symmetry reflecting the hexagonal symmetry of GaN thin films subjected to Berkovich nanoindentation. And, the evolution of CL impressions of such defects with increasing the indentation loads is displayed in Fig. 2. By increasing the indentation loading, the central zone becomes larger and more perturbed, accompanied by the shorter and very dark arms displaying between the double arms. The sizes of dark regions in CL images are about 2, 4, and 7 μm for the indentation loads of 10, 50, and 100 mN, respectively.

From CL observations, it displays as two well-separated zones: (i) a strongly perturbed central zone, appearing as a very dark zone with non-uniform distribution damage and (ii) six double arms, nearly parallel to axes separated by an angle of $\sim 60°$, confirming the hexagonal symmetry. From Fig. 2d, the CL images of Berkovich nanoindentations showed a very well-defined rosette structure with the hexagonal symmetry, which extends to the distance as double arms in directions at $\sim 60°$ intervals (namely; $\pm[11\bar{2}0]$, $\pm[2\bar{1}\bar{1}0]$, and $\pm[1\bar{2}10]$). The dark spots are visible in each arm; they correspond to the emergences of dislocations on the surface which act as non-radiative recombination centers and therefore quench locally the luminescence in the deformed areas. In addition, the intensity of the near-gap CL emission from GaN thin films is dramatically suppressed after Berkovich nanoindentation due to the induced defects/dislocations. Despite the star-of-David-like rosettes have been investigated around the larger indentation loading [16, 17]; however, such details could not be clearly resolved for the lower condition in our present work.

It is interesting to note that CL imaging on the indented area of GaN thin films corresponding to the critical "pop-in" load revealed slightly detectable reduction in the CL emission intensity. Indeed, under such a lower indentation load of 10 mN, for which only a small percentage of plastic deformation was induced, CL imaging was able to distinguish between the indentations that had undergone certain degrees of plastic deformation (after "pop-in" event) and those that were purely in the elastic regime (before "pop-in" event). Consequently, an observable CL impression is only detected after the "pop-in" event. It is thus evidenced that the "pop-in" event involves the nucleation of slip in the deformation mechanisms.

In addition, according to the previously studies [10, 17], we note here that the critical applied indentation load for direct identification of the multiple "pop-in" events in *P–h* curve is not only dependent on the type of indenters used, but also even very much dependent on the test systems and the maximum indentation loads applied. Consequently, we reasonably deduce that these discrepancies are mainly owing to the various indentation methods used. For instance, the tip-surface contact configuration and stress distribution for the Berkovich indenter tip can be drastically different from that for the spherical one or Vickers-type indenters [10, 17, 18].

Returning to the multiple "pop-in" events, it should be noted that the phenomena have been observed previously in hexagonal structured sapphire [19], single-crystal bulk

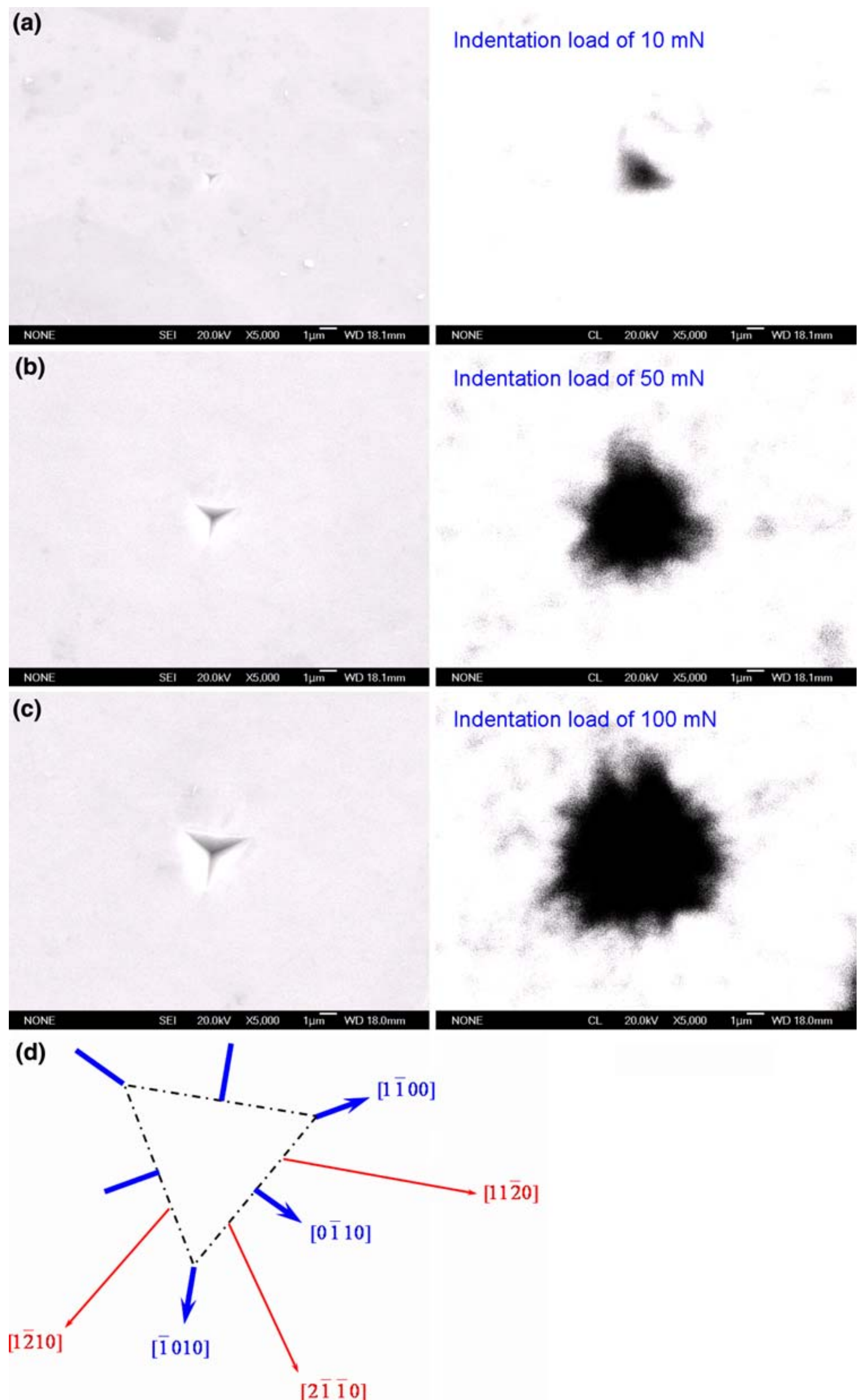

Fig. 2 Room temperature CL images (right figures) of indentation at loads of (**a**) 10, (**b**) 50, and (**c**) 100 mN. CL imaging conditions: electron beam energy = 20 keV, CL wavelength = 366 nm. Left figures: corresponding SE images. (**d**) Schema of an indentation figure as imaged by SEM/CL

ZnO [20], and GaN thin films [21]. On the other hand, materials with the cubic structure such as GaAs and InP are exhibited only single "pop-in" characteristic [22]. Nevertheless, the above discussions do suggest that multiple "pop-in" events indeed are specific features of materials with the hexagonal lattice structure and the geometry of the indenter tip may play an important role in determining the nanoindentation-induced mechanical responses. As a

result, in order to identify the deformation mechanisms specific to the Berkovich nanoindentation directly microstructures characteristics in the vicinity of indented area are needed. This plastic deformation process is complex and further studies will be necessary to delineate what happens to the material as the indenter penetrates into the surface. The nanoindentation-induced deformation mechanisms will be discussed in more detail with the aids of XTEM techniques in the following.

A bright-field XTEM image of GaN thin film after indented with an indentation load of 100 mN is shown in Fig. 3a. It clearly displays that, within this thin film, the deformation features underneath the indented spot are primarily manifested by dislocation activities. Namely the slip bands are aligning parallel to the {0001} basal planes all way down to the GaN thin film-sapphire substrate interface. It is also interesting to note that the heavily strained features in the vicinity of interface may not be just accidental artifacts resulted from sample preparation. It might be direct evidence for displaying that, because of the excellent interface epitaxy between thin film and substrate, the effects of nanoindentation have, in fact, extended into the sapphire substrate. Nevertheless, the slip bands (dark thick lines in the photograph) clearly indicate that during the indentation the rapidly increasing dislocations can glide collectively along the easy directions. Here, in addition to those aligning parallel to the interface of GaN thin film-sapphire along the (0001) basal planes, slip bands oriented at $\sim 60°$ to GaN surface can also be observed. The 60° slip bands, which are believed to originate from dislocations gliding along the $\{10\bar{1}1\}$ pyramidal planes, however, are distributing in much shallower regions near the contacting surface. It is indicative that much higher stress level is needed to activate this slip system as compared to the one along the basal planes.

In order to have a closer look at the dislocation activities immediately beneath the Berkovich indenter tip, a more detailed microstructures near the intersections of the two sets of slip bands are displayed in Fig. 3b. It clearly displays a typical microstructure of a heavily deformed material, characterized by features of very high density of dislocations. The distorted slip bands and the extremely high dislocation densities at the intersections indicate highly strained state of GaN thin films. Nevertheless, even at the submicron scale, no evidence of subsurface cracking and film fragmentation was observed. Furthermore, the selected area diffraction (data not shown here) of heavily damaged regions did not show evidence of newly formed phases either.

From the above-mentioned observations and discussion, it is apparent that, in the Berkovich indentation scheme, the primary deformation mechanism for GaN thin film is dislocation nucleation and propagation along the easy slip systems. Since the multiple "pop-in" events are usually observed after the permanent plastic deformation has occurred and two of the possible mechanisms, the deformation-induced phase transition [14] and fracture of thin films [23], were basically ruled out, the most likely mechanisms responsible for the multiple "pop-in" events appear to be associated with the activation of dislocations sources [24]. In this scenario, the

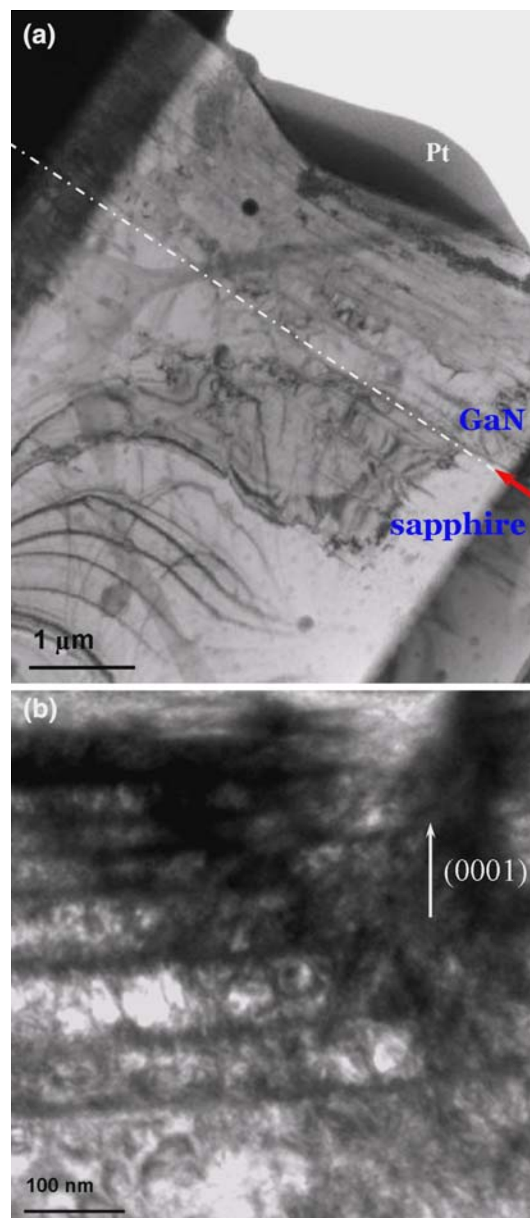

Fig. 3 (**a**) XTEM images of specimen after an indentation load to 100 mN: a lower magnification photograph showing the regions beneath the indent and part of the substrate. Notice that the basal plane slip bands propagate all way to the film-substrate interface and the stress field appears to extend into the substrate. (**b**) A close-up view of XTEM image of the heavily deformed region of GaN thin film, displaying that despite of being deformed heavily there is no evidence of crack formation

plastic deformation prior to the multiple "pop-in" events is associated with the individual movement of a small number of newly nucleated and pre-existing dislocations. As the number of dislocations is increased and entangled to each other, large shear stress is quickly accumulated underneath the indenter tip. When the local stress underneath the tip reaches some threshold level, a burst of collective dislocation movement on the easy slip systems is activated, resulting in a large release of local stress and a "pop-in" event on the loading segment of *P–h* curve. Each of these collective dislocation movements is reflected as a slip band in the indented microstructure as displayed in Fig. 3. Notice that, although the slip bands appeared to stop near the interface of GaN thin film-sapphire substrate, the released stress owing to this effect could extend deep into the sapphire substrate as mentioned above. Moreover, the narrow spacing of dense bands of defects and/or dislocations along the basal planes near GaN surface suggests that, in the later stage of indentation, a larger indentation load, such as the 100 mN applied in the present work, starts to activate the extensive slip bands along the $\sim 60^\circ$ pyramidal planes. The extensive interactions between the dislocations slipping along the two slip systems, therefore, confined the slip bands in a shallow regime, which, in turn, resulted in a heavily deformed and strain-hardened lattice structure. Finally, we note that the so-called "slip-stick" behavior [21], characterized by material "pile-ups" phenomena caused by interactions between the as-grown defects and the nanoindentation-induced dislocations, is not significantly here. Whether it is owing to the insignificant grown-in defect density of our GaN thin films or is related to the specific geometric shape of indenter tips used is not clear at present and further studies may be required to clarify this issue.

Conclusion

To summarize, a combination of nanoindentation, CL, FIB, and TEM techniques has been carried out to investigate the contact-induced structural deformation mechanisms in MOCVD-derived GaN thin films.

CL observations of nanoindentation show the very well-defined rosette structures with the hexagonal system. The rosette glide is characterized by the arms in $\pm[11\bar{2}0]$, $\pm[2\bar{1}\bar{1}0]$, and $\pm[1\bar{2}10]$ directions. The Berkovich nanoindentation-induced deformation acts as non-radiative recombination centers, which is confirmed by the reduction in the intensity of CL emission. In addition, CL imaging of indents displays to be a sensitive measure of the onset of slip since CL contrast of indents correlates well with the observation of multiple "pop-in" events. XTEM observations show that the prime deformation mechanisms in GaN thin films are the nucleation of slip on both the basal and pyramidal planes, rather than otherwise proposed stress-induced phase transformation or crack formation events. Finally, this study has significantly implications for the extent of contact-induced damage during fabrication of GaN-based optoelectronic devices.

Acknowledgments This work was partially supported by the National Science Council of Taiwan, under Grant no.: NSC97-2218-E-214-003. The authors like to thank Mr. Chia-Huang Li for his technical support.

References

1. J.H. Edgar (ed.), *Electronic Materials Information Service (EMIS) Data Reviews Series* (Institution of Electrical Engineers, London, 1994)
2. F.A. Ponce, D.P. Bour, Nature **386**, 351 (1997)
3. I. Zarudi, J. Zou, L.C. Zhang, Appl. Phys. Lett. **82**, 874 (2003)
4. C.R. Taylor, E.A. Stach, G. Salamo, A.P. Malshe, Appl. Phys. Lett. **87**, 073108 (2005)
5. B. Haberl, J.E. Bradby, S. Ruffell, J.S. Willams, P. Munroe, J. Appl. Phys. **100**, 013520 (2006)
6. S. Basu, M.W. Barsoum, A.D. Williams, T.D. Moustakas, J. Appl. Phys. **101**, 083522 (2007)
7. H. Wen, X. Wang, L. Li, J. Appl. Phys. **100**, 084315 (2006)
8. Y.B. Park, M.J. Dicken, Z.H. Xu, X.D. Li, J. Appl. Phys. **102**, 083507 (2007)
9. P.F. Yang, H.C. Wen, S.R. Jian, Y.S. Lai, S. Wu, R.S. Chen, Microelectron Reliab. **48**, 389 (2008)
10. S.R. Jian, T.H. Fang, D.S. Chuu, J. Electron. Mater. **32**, 496 (2003)
11. X.D. Li, B. Bhushan, Mater. Charact. **48**, 11 (2002)
12. W.C. Oliver, G.M. Pharr, J. Mater. Res. **7**, 1564 (1992)
13. D.F. Bahr, D.E. Kramer, W.W. Gerberich, Acta Mater. **46**, 3605 (1998)
14. J. Jang, M.J. Lance, S. Wen, T.Y. Tsui, G.M. Pharr, Acta Mater. **53**, 1759 (2005)
15. S. Ruffell, J.E. Bradby, N. Fujisawa, J.S. Williams, J. Appl. Phys. **101**, 083531 (2007)
16. M.H. Zaldivar, P. Fernández, J. Piqueras, Semicond. Sci. Technol. **13**, 900 (1998)
17. S.O. Kucheyev, J.E. Bradby, J.S. Williams, C. Jagadish, M. Toth, M.R. Phillips, M.V. Swain, Appl. Phys. Lett. **77**, 3373 (2000)
18. P. Kavouras, Ph. Komninou, Th. Karakostas, Thin Solid Films **515**, 3011 (2007)
19. R. Nowak, T. Sekino, S. Maruno, K. Niihara, Appl. Phys. Lett. **68**, 1063 (1996)
20. S.O. Kucheyev, J.E. Bradby, J.S. Williams, C. Jagadish, M.V. Swain, Appl. Phys. Lett. **80**, 956 (2002)
21. J.E. Bradby, S.O. Kucheyev, J.S. Williams, J.W. Leung, M.V. Swain, P. Munroe, G. Li, M.R. Phillips, Appl. Phys. Lett. **80**, 383 (2002)
22. J.E. Bradby, J.S. Williams, J.W. Leung, M.V. Swain, P. Munroe, Appl. Phys. Lett. **78**, 3235 (2001)
23. S.J. Bull, J. Phys. D: Appl. Phys. **38**, R393 (2005)
24. Y. Gaillard, C. Tromas, J. Woirgard, Philos. Mag. Lett. **83**, 553 (2003)